Application of Variational Mode Decomposition to FMCW Radar Interference Mitigation

Thilina Balasooriya
Clark Scholars Program (TTU)
Hamilton High School
Chandler, USA
tbalasooriya1@gmail.com

Prateek Nallabolu
Electrical and Computer Engineering
Texas Tech University
Lubbock, USA
prateek-reddy.nallabolu@ttu.edu

Changzhi Li
Electrical and Computer Engineering
Texas Tech University
Lubbock, USA
changzhi.li@ttu.edu

***Abstract*— As the automotive industry progresses towards implementing advanced driver-assistance systems (ADAS) and autonomous vehicles (AVs) that involve radars, the probability of radar interference between vehicles will increase tremendously in the future. To address this issue, novel interference mitigation methods for real-time interpretation are necessary. This work presents an evaluation of variational mode decomposition (VMD) based baseband reconstruction for interference mitigation in frequency-modulated continuous-wave (FMCW) radars using a MATLAB simulation. The VMD algorithm is applied to decompose the interference added baseband signal into multiple frequency components. The interference data samples in the baseband signal are removed from the interference-free data samples. The authors find that VMD has potential for this application, with the simulation results indicating an improvement in the noise floor of the recovered interference-free baseband signal.**

Keywords—Automotive radar, frequency-modulated continuous-wave (FMCW) radar, radar interference, variational mode decomposition (VMD).

I. Introduction

With the increasing interest for advanced driver-assistance systems (ADAS) and autonomous vehicles (AV), frequency-modulated continuous-wave (FMCW) radars have emerged as a key sensing modality due to their all-weather detection capability, low cost, and wide coverage [1], [2]. State-of-the-art millimeter-wave (mmWave) automotive radars have been employed for ADAS functionalities such as adaptive cruise control (ACC), blind-spot detection (BSD), and collision avoidance systems, to mention a few. Typically, each vehicle is equipped with multiple radars that serve various ADAS functions. With the increasing number of automotive radars on the road, interference among these radars needs to be addressed and tackled.

The main manifestations of interference in FMCW radars are the occurrence of ghost targets and elevated noise floor, leading to reduced sensitivity in detecting weak targets. Several methods have been proposed to address interference mitigation in FMCW radar systems. In [3], a frequency hopping technique was proposed in which the operating frequency of the FMCW radar was randomly assigned in the 76-81 GHz band, such that it was mathematically improbable for two radars to operate in the same frequency sub-band. However, this is not foolproof, and as the environments become more crowded, random frequency hopping will be a less viable solution. Time-domain zeroing of interfered samples was proposed in [4], in which the interfered section of the baseband signal was identified by applying an amplitude threshold and replacing the corresponding data samples with zeros to get rid of the interference. This method compromises the accuracy by completely ignoring a section of data, which is not the optimal desired solution. To combat this issue, several works were proposed that estimate the interference pattern using techniques such as mathematical analysis [5] and adaptive noise cancellation [6]. However, the works mentioned above [5], [6] require complex baseband architecture radar for optimal performance. Since the interference removal can be considered as a classical denoising problem, sparse reconstruction techniques such as orthogonal matching pursuit (OMP) and Bayesian learning were used in [7], [8], respectively. If the number of interference-generated data samples increases, the sparse reconstruction methods will fail to recover the interference-free signal. A recurrent neural network (RNN) that implements a self-attention model was proposed in [9], which predicts how well the target output attends to the baseband input. Convolution neural networks (CNN) based interference mitigation was proposed in [10], [11], where interference added range-Doppler (RD) frames were given as input, and the CNNs were trained to output the interference-free RD frame. However, to generate an extensive training set that included all the real-world interference patterns would be an impossible task.

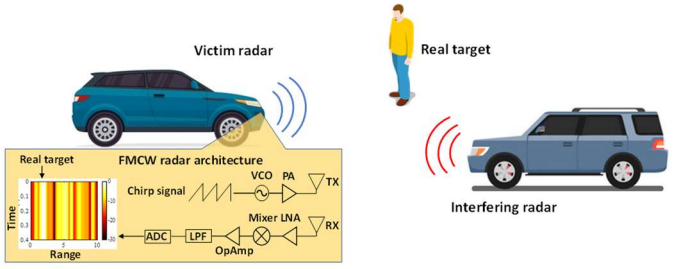

Fig. 1. Graphical illustration of the interference scenario in an automotive FMCW radar caused by a nearby radar.

This paper performs a feasibility study on the application of variational mode decomposition (VMD) for interference mitigation in FMCW radars. MATLAB simulations were performed to evaluate the performance of VMD to remove interference generated baseband data for various interference

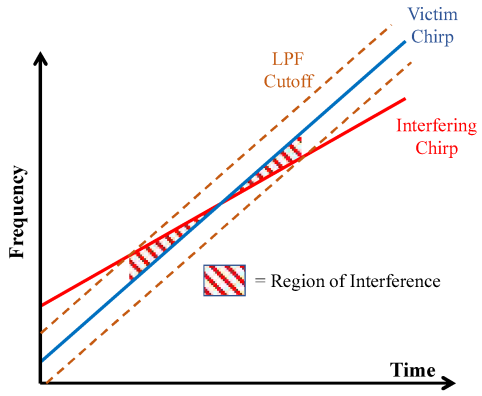

Fig. 2. The region of interference between the victim chirp and the interference chirp.

patterns. Unlike existing methods, the proposed VMD approach doesn't require identifying the interference-affected data samples beforehand. The rest of this work is organized as follows: Section II presents the theory of FMCW radar interference and VMD. Section III discusses the MATLAB simulation setup and the obtained simulation results. Finally, conclusions are drawn in Section IV.

II. Theory

A. FMCW Interference Model

Fig. 1 shows a real-world scenario of the interference caused in an automotive radar by a surrounding radar. An automotive FMCW radar transmits a chirp signal characterized by a bandwidth B and chirp duration T. This chirp signal gets reflected off a target, undergoes amplification on the radar's receiver chain, and upon de-ramping generates an intermediate frequency (IF) signal (also referred to as baseband signal). The de-ramping operation refers to the mixing of the received signal with the transmitted chirp signal. The time delay between the transmitted and received chirp signal translates to the frequency of the baseband signal, referred to as beat frequency. The generated beat frequency is unique depending on the range of the target. The generated baseband signal is passed through a low-pass filter (LPF) and then further amplified before it is digitized for further signal processing. Ideally, the cut-off frequency of the LPF is chosen based on the maximum detectable range of the radar, which in turn dictates the maximum beat frequency generated by the de-ramping operation. The baseband signal generated at the output of the LPF can be mathematically represented as:

$$S_{\mathrm{IF}}(t) = H_{\mathrm{LPF}}(t) \times Re\left[S_{\mathrm{TX}}(t) \times S'_{\mathrm{RX}}(t)\right], \qquad (1)$$

where t represents the so-called fast-time, Re[.] denotes the real part of the complex number, and $(.)'$ denoted complex conjugate operation. $S_{\mathrm{TX}}(t)$, $S_{\mathrm{RX}}(t)$, and $S_{\mathrm{IF}}(t)$ represent the transmitted and received chirp signal, and the generated baseband signal, respectively. The transfer function on the LPF is represented as $H_{\mathrm{LPF}}(t)$. $H_{\mathrm{LPF}}(t)$ can be considered as unity for the chirp signals reflected off a true target because the generated beat frequencies lie within the cut-off frequency of the LPF. In the presence of an interfering radar transmitting a chirp signal

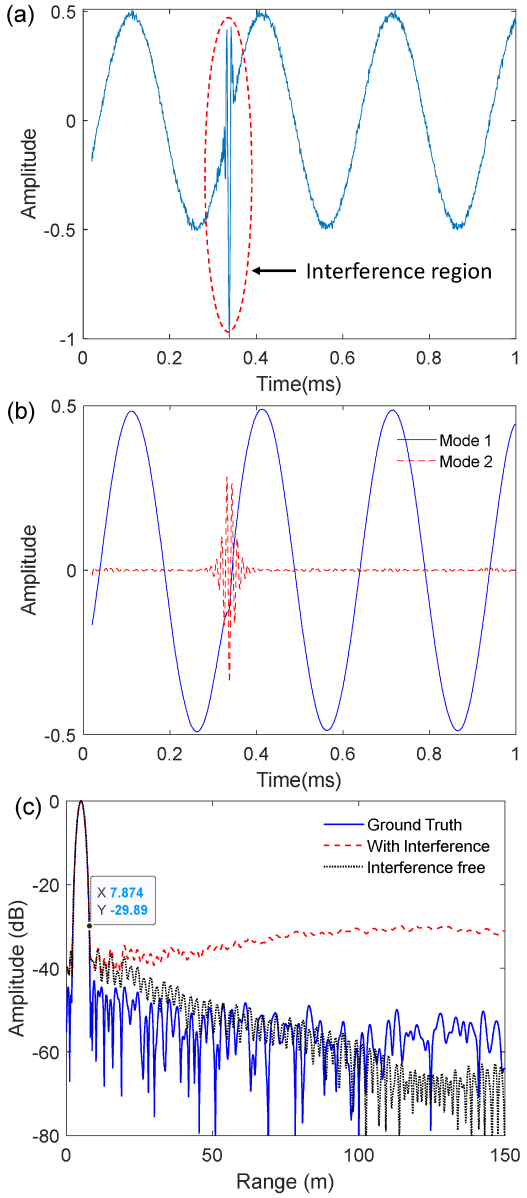

Fig. 3. (a) The generated interference added baseband signal, (b) VMD decomposition output modes, and (c) obtained range map for experiment scenario 1.

$S^*_{\mathrm{TX}}(t)$, the interference added baseband signal $S^*_{\mathrm{IF}}(t)$ generated after the LPF of the victim radar is given as:

$$S^*_{\mathrm{IF}}(t) = S_{\mathrm{IF}}(t) + H_{\mathrm{LPF}}(t) \times Re\left[S_{\mathrm{TX}}(t) \times S'_{\mathrm{TX}}(t - \tau^*)\right], \qquad (2)$$

where τ^* represents the one-way signal propagation delay due to the arbitrary distance between the victim and interference radar. The similarity between the slope (bandwidth/time) of the victim radar chirp and the interfering radar chirp and the bandwidth of the LPF determine the impact of the interference on the generated baseband signal. The more identical the slopes, the more baseband data samples affected by the interfering radar. Also, the higher the LPF bandwidth, the greater the interference's impact on the generated baseband data. Fig. 2 shows the impact of the cut-off frequency of the

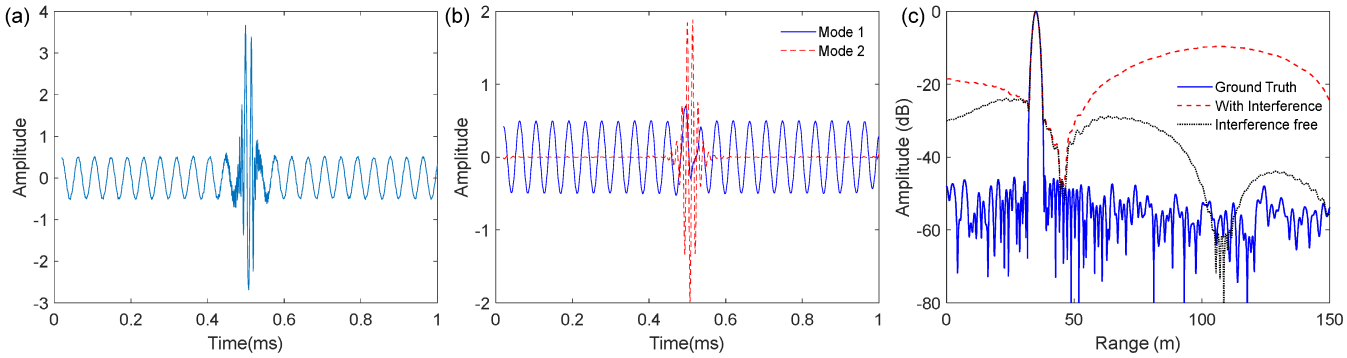

Fig. 4. (a) The generated interference added baseband signal, (b) VMD decomposition output modes, and (c) obtained range map for experiment scenario 2.

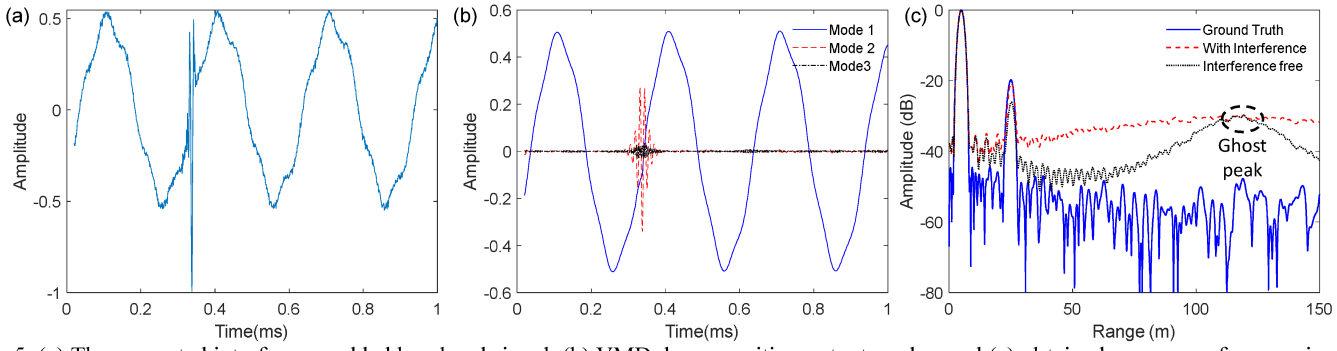

Fig. 5. (a) The generated interference added baseband signal, (b) VMD decomposition output modes, and (c) obtained range map for experiment scenario 3.

LPF on the region of interference caused due to the interfering radar. It should also be noted that the similarity between the slopes of the victim and the interference chirp also affects the region of interference.

B. Variational Mode Decomposition

Variational mode decomposition algorithm decomposes a non-stationary signal into consequent variational mode functions (VMFs) [12]. Each VMF is characterized by a center frequency and bandwidth. VMD consists of three major steps: computing the analytic signal for each mode μ_k using Hilbert transform, shift each mode's frequency spectrum to baseband by using an exponential tuned to the mode's estimated center frequency, and then perform Gaussian smoothing to estimate the bandwidth. The number of VMFs is directly inputted to the algorithm using the parameter k, while the parameter α decides the bandwidth and center frequency of each VMF. To summarize, the higher the value of α, the narrower the bandwidth of each mode, and the center frequency increases with the mode number. Additional parameters include noise tolerance which can be set to zero for optimal results.

From Fig. 2, it can be seen that the interference region is very narrow and results in high-frequency components in the baseband signal within the interference region. Using VMD, the interference added baseband signal can be decomposed into multiple modes such that the highest mode consists of the interference data samples, while the lower modes represent the baseband signal components generated by the true targets.

III. Simulation Results

Based on the interference model presented in Section II-A, a simulation setup was created in MATLAB software. To ease the computational load, the operating band of the FMCW radars was limited to 1-500 MHz. The victim radar was configured with a bandwidth of 100 MHz (200-300 MHz) and a chirp duration of 1 ms. The cut-off frequency of the LPF in the victim radar was set to 50 kHz. In the first scenario, the victim radar was configured with a bandwidth of 130 MHz (190-320 MHz) and a chirp duration of 1 ms. A single true target was considered at a distance of 3 m, and the signal strength of the interfering chirp was considered to be three times that of the reflections from the true target. This reflects a real-world scenario, where the interference chirp has to travel one way, undergoing lower path loss and thus having higher signal strength at the receiver port of the victim radar, compared to the reflections from true targets. Fig. 3(a) demonstrates the baseband signal with added interference. The signal-to-noise (SNR) was set to 30 dB. The VMD algorithm was applied to the interference added baseband data with the parameters set to $k = 2$ and $\alpha = 5000$. With $k = 2$, the signal was decomposed into two VMFs, where the first VMF corresponds to the interference-free baseband signal. Fig. 3(b) shows the decomposed VMF modes 1 and 2. Mode 1 represents the interference-free baseband, and mode 2 represents the interference plus noise. Fig. 3(c) shows a comparison of the range maps of the interference added and interference-free baseband signals with the ground truth (ideal scenario with no interference). The increase in the noise floor of the signal with

added interference and the significant improvement in the noise floor in the interference-free range map can be observed.

In the second scenario, the FMCW parameters of the interference radar were set to a bandwidth of 100 MHz (195-305 MHz) and a chirp duration of 1ms. Due to the high correlation between the victim and interference chirp, the interference region will be broader in this scenario. A true target at a distance of 35 m was considered, and the ratio of signal strength of the interference signal to that of the reflection from the true target was set to ten. The VMD parameters were unchanged. As seen in Fig. 4(a), the interference region was broader, and the interference samples' amplitude was much higher than scenario 1. As the beat frequency generated due to the true target at 35 m is higher, the decomposed mode 1 in Fig. 4(b), representing the interference-free baseband signal, still has some distortion. However, the range map for the interference-free baseband data has a much lower noise floor than the interference added range map, as shown in Fig. 4(c).

In the third simulation scenario, two real targets were considered at 5 m and 25 m. The bandwidth and time duration of the interference chirp was set to 130 MHz (190-320 MHz) and 1 ms, respectively. The VMD algorithm was applied to decompose the baseband signal shown in Fig. 5(a) into three VMFs by setting k to 3. However, since $\alpha = 3$ represents a moderate bandwidth constraint, both the target responses were decomposed into mode 1, as seen in Fig. 5(b). Ideally, for targets at a farther distance, their response would be decomposed into mode 2, and summing mode 1 and 2 output would provide an estimate of the interference-free baseband signal. From the range maps shown in Fig. 5(c), it can be observed that the noise floor in the interference-free case was improved until the 100 m range. However, around 125 m, the noise floor hits a peak and appears like a ghost target. In this scenario, given the correct set of VMD parameters, the ghost peak could be avoided.

The VMD approach poses few drawbacks. The recovery of the interference-free baseband signal is dependent on various factors like the similarity between the victim and interference chirp slopes, the distance of the true targets, the number of true targets, and the signal strength of the interference chirp. Different scenarios might require different VMD parameters to obtain the optimal interference-free baseband reconstruction. Therefore, it is necessary to either find a standardized set of parameters that work almost universally or create an algorithm to decide the appropriate VMD parameters given the situation.

IV. Conclusion

As radar-based automotive features and self-driving cars become more prevalent, the probability of radar interference will increase, causing many potential driving hazards. A radar interference mitigation technique based on a variational mode decomposition approach was evaluated using MATLAB simulation to address this need. The use of VMD for removing interference-affected samples from the baseband signal has proven promising. The recovered interference-free baseband signals exhibited improvement of the noise floor. Future work includes creating a standardized set of VMD parameters for any interference scenario and addressing the issue of ghost peaks.

Acknowledgment

The authors wish to acknowledge the National Science Foundation (NSF) for funding support under grant ECCS-2028863 and ECCS-1808613.

References

[1] M. Vossiek, P. Heide, M. Nalezinski, and V. Magori, "Novel FMCW radar system concept with adaptive compensation of phase errors," *1996 26th European Microwave Conference*, 1996, pp. 135-139.

[2] Yeonghwan Ju, Youngseok Jin, and Jonghun Lee, "Design and implementation of a 24 GHz FMCW radar system for automotive applications," *2014 International Radar Conference*, 2014, pp. 1-4.

[3] C. Aydogdu et al., "Radar interference mitigation for automated driving: Exploring proactive strategies," in *IEEE Signal Processing Magazine*, vol. 37, no. 4, pp. 72-84, July 2020.

[4] G. M. Brooker, "Mutual Interference of Millimeter-Wave Radar Systems," in *IEEE Transactions on Electromagnetic Compatibility*, vol. 49, no. 1, pp. 170-181, Feb. 2007.

[5] J. Bechter, K. D. Biswas, and C. Waldschmidt, "Estimation and cancellation of interferences in automotive radar signals," *2017 18th International Radar Symposium* (*IRS*), 2017, pp. 1-10.

[6] F. Jin and S. Cao, "Automotive Radar Interference Mitigation Using Adaptive Noise Canceller," in *IEEE Transactions on Vehicular Technology*, vol. 68, no. 4, pp. 3747-3754, April 2019.

[7] A. Correas-Serrano and M. A. Gonzalez-Huici, "Sparse Reconstruction of Chirplets for Automotive FMCW Radar Interference Mitigation," *2019 IEEE MTT-S International Conference on Microwaves for Intelligent Mobility* (*ICMIM*), 2019, pp. 1-4.

[8] S. Chen, J. Taghia, U. Kühnau, T. Fei, F. Grünhaupt, and R. Martin, "Automotive Radar Interference Reduction Based on Sparse Bayesian Learning," *2020 IEEE Radar Conference* (*RadarConf20*), 2020, pp. 1-6.

[9] J. Mun, S. Ha, and J. Lee, "Automotive Radar Signal Interference Mitigation Using RNN with Self Attention," *2020 IEEE International Conference on Acoustics, Speech and Signal Processing* (*ICASSP*), 2020, pp. 3802-3806.

[10] J. Fuchs, A. Dubey, M. Lübke, R. Weigel, and F. Lurz, "Automotive Radar Interference Mitigation using a Convolutional Autoencoder," *2020 IEEE International Radar Conference* (*RADAR*), 2020, pp. 315-320.

[11] J. Rock, M. Toth, E. Messner, P. Meissner, and F. Pernkopf, "Complex Signal Denoising and Interference Mitigation for Automotive Radar Using Convolutional Neural Networks," *2019 22th International Conference on Information Fusion* (*FUSION*), 2019, pp. 1-8.

[12] K. Dragomiretskiy and D. Zosso, "Variational Mode Decomposition," in *IEEE Transactions on Signal Processing*, vol. 62, no. 3, pp. 531-544, Feb.1, 2014.